

Structure Elucidation of the Adducts Formed by Fjord Region Dibenzo[*a,l*]pyrene-11,12-dihydrodiol 13,14-Epoxides with Deoxyguanosine

Kai-Ming Li,[†] Mathai George,[§] Michael L. Gross,[§] Cheng-Huang Lin,^{||}
Ryszard Jankowiak,[⊥] Gerald J. Small,^{||,⊥} Albrecht Seidel,[‡] Heiko Kroth,[∇]
Eleanor G. Rogan,[†] and Ercole L. Cavalieri^{*,†}

Eppley Institute for Research in Cancer and Allied Diseases, University of Nebraska Medical Center, 986805 Nebraska Medical Center, Omaha, Nebraska 68198-6805, Department of Chemistry, Washington University, One Brookings Drive, St. Louis, Missouri 63130-4899, Department of Chemistry and Ames Laboratory-U.S. Department of Energy, Iowa State University, Ames, Iowa 50011, and Institute of Toxicology, University of Mainz, Mainz, Germany

Received October 21, 1998

(±)-*anti*-Dibenzo[*a,l*]pyrene-11,12-dihydrodiol 13,14-epoxide {(±)-*anti*-DB[*a,l*]PDE} was reacted with deoxyguanosine (dG) in dimethylformamide at 100 °C for 30 min, and two sets of adducts were isolated: a mixture of (±)-*anti-cis*- & -*trans*-N²dG (43%) and a mixture of (±)-*anti-cis*- & -*trans*-N7Gua (45%). Both are mixtures of four stereoisomers that cannot be separated by HPLC. Similarly, (±)-*syn*-DB[*a,l*]PDE was reacted with dG under the same conditions, and (±)-*syn-cis*- & -*trans*-N²dG (38%) and (±)-*syn-cis*- & -*trans*-N7Gua (59%) were obtained. The structures of the adducts were determined by a combination of NMR and fast atom bombardment mass spectrometry. By reacting (−)-*anti*-DB[*a,l*]PDE or (+)-*syn*-DB[*a,l*]PDE with dG under the same conditions, however, optically pure N²dG and N7Gua isomers were obtained: (−)-*anti-cis*-N²dG (12%), (−)-*anti-trans*-N²dG (17%), (−)-*anti-trans*-N7Gua (43%), (+)-*syn-cis*-N²dG (7%), (+)-*syn-trans*-N²dG (3%), (+)-*syn-cis*-N7Gua (36%), and (+)-*syn-trans*-N7Gua (22%). The structures of the optically pure adducts were assigned by NMR. *syn*- and *anti*-DB[*a,l*]PDE–N²dG adducts can be distinguished by fluorescence line-narrowing spectroscopy (FLNS). Moreover, distinction between *cis*- and *trans*-stereochemistry of the adducts is also straightforward by FLNS, because the FLN spectra for the four DB[*a,l*]PDE–N²dG adducts, *anti-cis*, *anti-trans*, *syn-cis*, and *syn-trans*, are spectroscopically unique.

Introduction

Polycyclic aromatic hydrocarbons (PAH)¹ are activated by two major pathways, one-electron oxidation with formation of radical cations and monooxygenation with formation of diol epoxides, or, more frequently, a combination of both pathways (1, 2). In DNA, the Ade and Gua bases are the most frequent targets of metabolically activated PAH. Electrophilic attack by PAH radical cations and diol epoxides at the N-3 and N-7 of Ade or the N-7 and sometimes C-8 of Gua leads to formation of depurinating adducts that are lost from DNA by cleavage of the glycosidic bond (2). When reaction occurs at the exocyclic amino group of deoxyguanosine (dG) or deoxy-

adenosine (dA), the adducts obtained are stable and remain in DNA.

Investigating the postulated mechanism of metabolic activation of dibenzo[*a,l*]pyrene² (DB[*a,l*]P) requires reference adducts formed by DB[*a,l*]P radical cation and by fjord region DB[*a,l*]P-11,12-dihydrodiol 13,14-epoxides (DB[*a,l*]PDE). Synthesis of DB[*a,l*]P adducts by one-electron oxidation was already reported (3, 4). In addition, adducts formed by DB[*a,l*]PDE with dA were recently synthesized (5). In this article, we report the synthesis and structure elucidation of the adducts formed by reaction of DB[*a,l*]PDE with dG.

Stable and depurinating adducts of DB[*a,l*]P were obtained by microsomal activation of this compound in the presence of DNA (6). Furthermore, stable dA and dG adducts of DB[*a,l*]PDE have been identified in cell culture, indicating that DB[*a,l*]P is stereoselectively converted to the (+)-*syn*- and (−)-*anti*-DB[*a,l*]PDE with 11*S*,12*R*,13*S*,14*R*- and 11*R*,12*S*,13*S*,14*R*-configurations, respectively (7, 8).

Fluorescence line-narrowing spectroscopy (FLNS) can be used for fingerprint identification of various PAH–DNA adducts and PAH metabolites (9–12), and the combination of FLNS and non-line-narrowing (NLN) fluorescence spectroscopy provides conformational information (13–16). Spectral characterization of DB[*a,l*]PDE–N²dG and DB[*a,l*]PDE–N⁶dA standard adducts is

* To whom correspondence should be addressed.

† University of Nebraska Medical Center.

§ Washington University.

|| Department of Chemistry, Iowa State University.

⊥ Ames Laboratory-U.S. Department of Energy, Iowa State University.

‡ University of Mainz.

∇ Present address: Laboratory of Bioorganic Chemistry, National Institute of Diabetes and Digestive and Kidney Diseases, NIH, Bethesda, MD 20892.

¹ Abbreviations: CAD, collisionally activated decomposition; COSY, two-dimensional chemical shift correlation spectroscopy; dA, deoxyadenosine; DB[*a,l*]P, dibenzo[*a,l*]pyrene; DB[*a,l*]PDE, dibenzo[*a,l*]pyrene-11,12-dihydrodiol 13,14-epoxide(s); dG, deoxyguanosine; DMF, dimethylformamide; FAB MS, fast atom bombardment mass spectrometry; FLNS, fluorescence line-narrowing spectroscopy; NLN, non-line-narrowing; PAH, polycyclic aromatic hydrocarbon(s).

² IUPAC systematic name: dibenzo[*def,p*]chrysene.

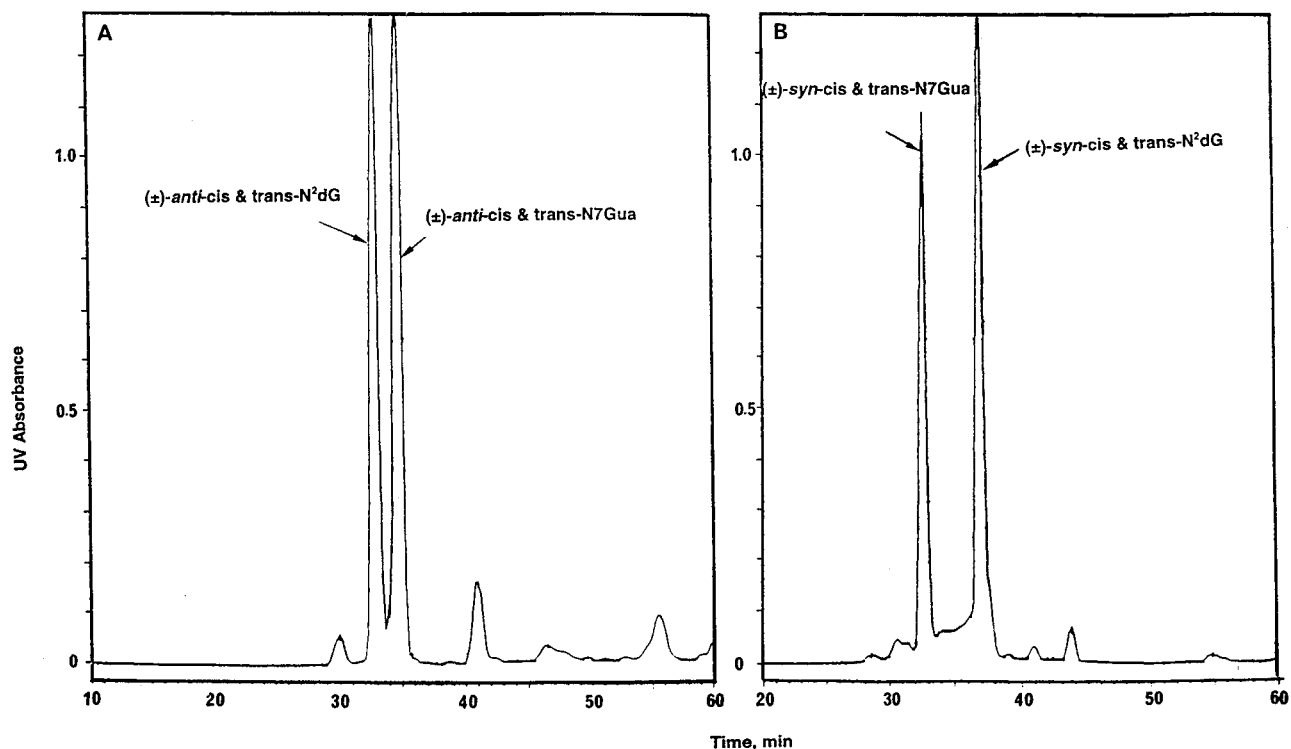


Figure 1. HPLC (CH₃CN/H₂O gradient) profile of products obtained by reaction of (A) (±)-*anti*-DB[a,l]PDE with dG and (B) (±)-*syn*-DB[a,l]PDE with dG.

essential for identification of adducts derived from *syn*- and *anti*-DB[a,l]PDE and provides the necessary reference information for studying DB[a,l]PDE-DNA adducts formed in vitro and in vivo. In this article, we also report the characterization of *anti-trans*-, *anti-cis*-, *syn-trans*-, and *syn-cis*-DB[a,l]PDE-N²dG adducts by FLNS. The results obtained for the corresponding DB[a,l]PDE-N⁶-dA adducts will be published elsewhere (17). Differences in the FLN spectra for the four N²dG adducts provide a means for selective, unambiguous identification of the four adducts after their formation in biological systems.

Experimental Section

Caution. DB[a,l]PDE are hazardous chemicals and were handled according to NIH guidelines (18).

General Procedures. All of the procedures for UV, NMR, fast atom bombardment mass spectrometry (FAB MS), and HPLC were the same as previously described (5). The spectra of the (±)-*anti-cis*- & -*trans* and (±)-*syn-cis*- & -*trans* adducts were recorded in Me₂SO-*d*₆ at 25 °C, whereas the spectra of the (-)-*anti* and (+)-*syn* adducts were recorded in Me₂SO-*d*₆/D₂O at 25 °C. The procedure for FLNS analysis of DB[a,l]PDE-N²-dG adducts was the same as that described in previous publications (16, 17, 19).

Chemicals. (±)-*anti*-DB[a,l]PDE and (±)-*syn*-DB[a,l]PDE were obtained from ChemSyn Science Laboratories (Lenexa, KS). (-)-*anti*-DB[a,l]PDE and (+)-*syn*-DB[a,l]PDE were synthesized as previously described (20, 21). The dG was purchased from Aldrich (Milwaukee, WI) and was desiccated over P₂O₅ under vacuum at 110 °C for 48 h prior to use. Commercially available dimethylformamide (DMF; Aldrich) was purified by refluxing over CaH₂, followed by distillation under vacuum and was stored over 4-Å molecular sieves under argon.

Chemical Synthesis of DB[a,l]PDE Adducts. The reaction of (±)-*anti*-DB[a,l]PDE is described here as an example. The same methods were used for reaction of the other DB[a,l]PDE. (±)-*anti*-DB[a,l]PDE (5 mg, 0.0142 mmol) was dissolved in 1 mL of dry DMF at room temperature under argon. The dG (35

Table 1. Adducts Obtained by Reaction of (±)-*anti*-, (-)-*anti*-, (±)-*syn*-, or (+)-*syn*-DB[a,l]PDE with dG in DMF at 100 °C for 30 min

product	yield (%)
(±)- <i>anti-cis</i> - & - <i>trans</i> -N ² dG	43
(±)- <i>anti-cis</i> - & - <i>trans</i> -N7Gua	45
(±)- <i>syn-cis</i> - & - <i>trans</i> -N ² dG	38
(±)- <i>syn-cis</i> - & - <i>trans</i> -N7Gua	59
(-)- <i>anti-cis</i> -N ² dG	12
(-)- <i>anti-trans</i> -N ² dG	17
(-)- <i>anti-trans</i> -N7Gua ^a	43
(+)- <i>syn-cis</i> -N ² dG	7
(+)- <i>syn-trans</i> -N ² dG	3
(+)- <i>syn-cis</i> -N7Gua	36
(+)- <i>syn-trans</i> -N7Gua	22

^a Only trace amounts of (-)-*anti-cis*-N7Gua were obtained.

mg, 0.133 mmol) was added to the above solution, and the reaction was carried out at 100 °C for 30 min. DMF was then removed under vacuum; the residue was dissolved in Me₂SO/CH₃OH (1:1) and analyzed by HPLC by using a CH₃CN/H₂O gradient (Figure 1A) (5). Purification of all adducts was conducted by preparative HPLC by using a CH₃CN/H₂O gradient, followed by isocratic elution with CH₃OH/H₂O (5). The purity of all adducts after preparative HPLC separations was independently checked by analytical HPLC in the two solvent systems, CH₃CN/H₂O and CH₃OH/H₂O. The adducts were isolated from the reaction of DB[a,l]PDE with dG in yields ranging from 3% to 59% (Table 1).

(±)-*anti*-11,12,13-Trihydroxy-14-N²dG-11,12,13,14-tetrahydro-DB[a,l]P [(±)-*anti-cis*- & -*trans*-N²dG]: UV λ_{max} 243, 277, 288, 298, 330, 343 nm; ¹H NMR δ 3.93 (m, 1H, 4'-H), 4.11–4.17 (m, 2H, 12-H, 13-H), 4.32 (m, 1H, 3'-H), 4.87 (bs, 1H, 11-H), 5.35–5.60 (m, 3H, 3'-OH, 5'-OH, 12-OH, can be exchanged with D₂O), 6.05 (bs, 1H, 1'-H), 6.10 (d, 1H, 11-OH, can be exchanged with D₂O), 6.57 (s, 1H, 13-OH, can be exchanged with D₂O), 6.95 (dd, 1H, 2-H, J_{1,2} = 7.5 Hz, J_{2,3} = 6.5 Hz), 7.41 (dd, 1H, 3-H, J_{2,3} = 6.5 Hz, J_{3,4} = 8.5 Hz), 7.48 (bd, 1H, 14-H, J_{13,14} = 2.0 Hz), 7.95 [s, 1H, 8-H(Gua)], 7.99 (d, 1H, 1-H, J_{1,2} = 7.5 Hz), 8.02 (t, 1H, 6-H, J_{5,6} = 8.0 Hz, J_{6,7} = 7.5 Hz), 8.15 (dd, 2H, 8-H, 9-H, J_{8,9} = 9.5 Hz), 8.22 [s, 1H, 2-NH(Gua), can be

exchanged with D₂O], 8.25 (d, 1H, 7-H, $J_{6,7} = 7.5$ Hz), 8.53 (s, 1H, 10-H), 8.61 (d, 1H, 4-H, $J_{3,4} = 8.5$ Hz), 8.88 (d, 1H, 5-H, $J_{5,6} = 8.0$ Hz); FAB MS [M + H]⁺ C₃₄H₃₀N₅O₇ calcd 620.2145, obsd 620.2129.

(±)-**anti-11,12,13-Trihydroxy-14-N7Gua-11,12,13,14-tetrahydro-DB[a,]P** [(±)-**anti-cis- & -trans-N7Gua**]: UV λ_{\max} 241, 277 (sh), 288, 296 (sh), 331, 343 nm; ¹H NMR δ 3.92 (d, 1H, 12-H, $J_{12,13} = 6.5$ Hz), 4.22 (dd, 1H, 13-H, $J_{12,13} = 6.5$ Hz, $J_{13,14} = 6.0$ Hz), 4.97 (bs, 1H, 11-H), 5.32 (bs, 1H, 11-OH, can be exchanged with D₂O), 5.40 (bs, 1H, 13-OH, can be exchanged with D₂O), 5.54 (bs, 1H, 12-OH, can be exchanged with D₂O), 6.55 (bs, 1H, 14-H), 6.90 [bs, 2H, 2-NH₂(Gua), can be exchanged with D₂O], 7.22 (bs, 1H, 2-H), 7.63 (bs, 1H, 3-H), 7.70 (d, 1H, 1-H, $J_{1,2} = 8.0$ Hz), 7.95 [s, 1H, 8-H(Gua)], 8.05 (dd, 1H, 6-H, $J_{5,6} = 8.0$ Hz, $J_{6,7} = 7.5$ Hz), 8.17 (d, 1H, 9-H, $J_{8,9} = 9.0$ Hz), 8.21 (d, 1H, 8-H, $J_{8,9} = 9.0$ Hz), 8.28 (d, 1H, 7-H, $J_{6,7} = 7.5$ Hz), 8.35 (s, 1H, 10-H), 8.89 (bs, 1H, 4-H), 8.99 (d, 1H, 5-H, $J_{5,6} = 8.0$ Hz); FAB MS [M + H]⁺ C₂₉H₂₂N₅O₄ calcd 504.1672, obsd 504.1686.

(±)-**syn-11,12,13-Trihydroxy-14-N²dG-11,12,13,14-tetrahydro-DB[a,]P** [(±)-**syn-cis- & -trans-N²dG**]: UV λ_{\max} 241, 278, 288, 296, 329, 342 nm; ¹H NMR δ 3.47 (bs, 1H, 4'-H), 3.75 (bs, 2H, 12_a-H, 12_b-H), 4.50–4.57 (m, 2H, 13_a-H, 13_b-H), 4.88 (bs, 2H, 11_a-H, 11_b-H), 5.21–5.31 (m, 4H, 3'-OH, 5'-OH, 12_a-OH, 12_b-OH, can be exchanged with D₂O), 5.95 (bs, 1H, 1'-H), 6.05–6.20 (m, 4H, 11_a-OH, 11_b-OH, 13_a-OH, 13_b-OH), 7.08–7.25 (m, 4H, 2_a-H, 2_b-H, 14_a-H, 14_b-H), 7.48 (dd, 1H, 3_b-H, $J_{2b,3b} = 7.0$ Hz, $J_{3b,4b} = 8.0$ Hz), 7.62 (dd, 1H, 3_a-H, $J_{2a,3a} = 7.0$ Hz, $J_{3a,4a} = 8.0$ Hz), 8.05–8.06 (m, 2H, 6_a-H, 6_b-H), 8.14 (m, 4H, 8_a-H, 9_a-H, 8_b-H, 9_b-H), 8.25 (d, 2H, 7_a-H, 7_b-H, $J_{6a,7a} = J_{6b,7b} = 7.5$ Hz), 8.42 [s, 1H, 8-H(Gua)], 8.50 (s, 2H, 10_a-H, 10_b-H), 8.60–8.63 (m, 2H, 1_a-H, 1_b-H), 8.70 (d, 1H, 4_b-H, $J_{3b,4b} = 8.0$ Hz), 8.87 (d, 1H, 4_a-H, $J_{3a,4a} = 8.0$ Hz), 8.91 (d, 1H, 5_b-H, $J_{5b,6b} = 8.0$ Hz), 8.96 (d, 1H, 5_a-H, $J_{5a,6a} = 8.0$ Hz); FAB MS [M + Na]⁺ C₃₉H₂₉N₅O₇Na calcd 642.1965, obsd 642.1949.

(±)-**syn-11,12,13-Trihydroxy-14-N7Gua-11,12,13,14-tetrahydro-DB[a,]P** [(±)-**syn-cis- & -trans-N7Gua**]: UV λ_{\max} 242, 280 (sh), 290, 297 (sh), 331, 344 nm; ¹H NMR δ 3.59 (bs, 1H, 12-H), 4.05 (m, 1H, 13_b-H), 4.26 (bs, 1H, 13_a-H), 4.85 (d, 1H, 11_b-H, $J_{11b,12b} = 10.0$ Hz), 4.91 (d, 1H, 11_a-H, $J_{11a,12a} = 8.0$ Hz), 5.15 (bs, 1H, 12_b-OH, can be exchanged with D₂O), 5.32 (bs, 1H, 12_a-OH, can be exchanged with D₂O), 5.94 (d, 1H, 11_b-OH, can be exchanged with D₂O, $J_{11b,11b-OH} = 6.5$ Hz), 6.02 (d, 1H, 11_a-OH, can be exchanged with D₂O, $J_{11a,11a-OH} = 6.0$ Hz), 6.13 (bs, 1H, 13_a-OH, can be exchanged with D₂O), 6.23 (bs, 1H, 13_b-OH, can be exchanged with D₂O), 6.34 (d, 1H, 14_b-H, $J_{13b,14b} = 4.5$ Hz), 6.68 (d, 1H, 14_a-H, $J_{13a,14a} = 3.5$ Hz), 6.78 [bs, 2H, 2_b-NH₂(Gua), can be exchanged with D₂O], 7.29 (dd, 1H, 2_b-H, $J_{1b,2b} = 7.5$ Hz, $J_{2b,3b} = 7.0$ Hz), 7.35–7.50 [bs, 2H, 2_a-NH₂(Gua), can be exchanged with D₂O], 7.36 (dd, 1H, 2_a-H, $J_{1a,2a} = 7.5$ Hz, $J_{2a,3a} = 7.0$ Hz), 7.61 (dd, 1H, 3_a-H, $J_{2a,3a} = 7.0$ Hz, $J_{3a,4a} = 8.0$ Hz), 7.91 [s, 1H, 8-H(Gua)], 7.97–8.04 (m, 2H, 6_a-H, 6_b-H), 8.04–8.30 (m, 4H, 8_a-H, 8_b-H, 9_a-H, 9_b-H), 8.24 (d, 2H, 7_a-H, 7_b-H, $J_{6a,7a} = J_{6b,7b} = 7.5$ Hz), 8.48–8.56 (m, 3H, 1_a-H, 10_a-H, 10_b-H), 8.67 (d, 1H, 4_b-H, $J_{3b,4b} = 8.5$ Hz), 8.80–8.87 (bs, 2H, 4_a-H, 5_b-H), 8.93 (d, 1H, 5_a-H, $J_{5a,6a} = 8.0$ Hz), 9.00 (d, 1H, 1_b-H, $J_{1b,2b} = 7.5$ Hz); FAB MS [M + Na]⁺ C₂₉H₂₁N₅O₄Na calcd 526.1491, obsd 526.1505.

(-)-**(11R,12S,13R)-Trihydroxy-(14R)-N²dG-11,12,13,14-tetrahydro-DB[a,]P** [(-)-**anti-cis-N²dG**]: UV λ_{\max} 243, 278 (sh), 288, 298, 328, 342 nm; ¹H NMR δ 3.92–3.96 (m, 1H, 4'-H), 4.13 (dd, 1H, 12-H, $J_{11,12} = 8.5$ Hz, $J_{12,13} = 2.0$ Hz), 4.32 (bs, 1H, 13-H), 4.52 (m, 1H, 3'-H), 5.06 (d, 1H, 11-H, $J_{11,12} = 8.5$ Hz), 6.36 (dd, 1H, 1'-H, $J_{1',2'} = 8.5$ Hz, $J_{1',2'} = 7.5$ Hz), 6.54 (d, 1H, 14-H, $J_{13,14} = 3.5$ Hz), 7.06 (dd, 1H, 2-H, $J_{1,2} = 8.5$ Hz, $J_{2,3} = 7.0$ Hz), 7.53 (dd, 1H, 3-H, $J_{2,3} = 7.0$ Hz, $J_{3,4} = 7.5$ Hz), 7.95 [s, 1H, 8-H(Gua)], 8.05 (dd, 1H, 6-H, $J_{5,6} = 7.5$ Hz, $J_{6,7} = 8.0$ Hz), 8.09–8.11 (m, 2H, 8-H, 9-H), 8.25 (d, 1H, 7-H, $J_{6,7} = 8.0$ Hz), 8.39 (s, 1H, 10-H), 8.49 (bd, 1H, 1-H, $J_{1,2} = 8.5$ Hz), 8.80 (d, 1H, 4-H, $J_{3,4} = 7.5$ Hz), 8.96 (d, 1H, 5-H, $J_{5,6} = 7.5$ Hz).

(-)-**(11R,12S,13R)-Trihydroxy-(14S)-N²dG-11,12,13,14-tetrahydro-DB[a,]P** [(-)-**anti-trans-N²dG**]: UV λ_{\max} 242,

262 (sh), 276 (sh), 285, 294, 327, 342 nm; ¹H NMR δ 3.44 (m, 1H, 12-H), 3.94 (m, 1H, 3'-H), 4.18 (m, 1H, 13-H), 5.09 (d, 1H, 11-H, $J_{11,12} = 8.5$ Hz), 6.00 (dd, 1H, 1'-H), 6.74 (d, 1H, 14-H, $J_{13,14} = 8.0$ Hz), 7.16 (dd, 1H, 2-H, $J_{1,2} = 8.5$ Hz, $J_{2,3} = 7.0$ Hz), 7.45–7.47 (m, 1H, 3-H), 7.69 [s, 1H, 8-H(Gua)], 8.03 (t, 1H, 6-H, $J_{5,6} = 7.5$ Hz, $J_{6,7} = 7.5$ Hz), 8.08–8.15 (m, 2H, 8-H, 9-H), 8.25 (d, 1H, 7-H, $J_{6,7} = 7.5$ Hz), 8.47 (s, 1H, 10-H), 8.64 (bd, 1H, 1-H, $J_{1,2} = 8.5$ Hz), 8.67 (d, 1H, 4-H, $J_{3,4} = 8.5$ Hz), 8.88 (d, 1H, 5-H, $J_{5,6} = 7.5$ Hz).

(-)-**(11R,12S,13R)-Trihydroxy-(14S)-N7Gua-11,12,13,14-tetrahydro-DB[a,]P** [(-)-**anti-trans-N7Gua**]: UV λ_{\max} 243, 278 (sh), 286, 295 (sh), 328, 342 nm; ¹H NMR δ 3.76 (d, 1H, 12-H, $J_{11,12} = 6.0$ Hz), 4.32 (dd, 1H, 13-H, $J_{13,14} = 6.0$ Hz, $J_{12,13} = 2.0$ Hz), 4.97 (d, 1H, 11-H, $J_{11,12} = 6.0$ Hz), 6.71 [s, 1H, 8-H(Gua)], 7.18 (d, 1H, 14-H, $J_{13,14} = 6.0$ Hz), 7.29 (bs, 1H, 2-H), 7.60 (bs, 1H, 3-H), 8.05 (t, 1H, 6-H, $J_{5,6} = 7.5$ Hz, $J_{6,7} = 7.5$ Hz), 8.16 (s, 2H, 8-H, 9-H), 8.27 (d, 1H, 7-H, $J_{6,7} = 7.5$ Hz), 8.38 (d, 1H, 1-H), 8.51 (s, 1H, 10-H), 8.83 (d, 1H, 4-H, $J_{3,4} = 6.0$ Hz), 8.95 (d, 1H, 5-H, $J_{5,6} = 7.5$ Hz).

(+)-**(11S,12R,13R)-Trihydroxy-(14R)-N²dG-11,12,13,14-tetrahydro-DB[a,]P** [(+)-**syn-cis-N²dG**]: UV λ_{\max} 228, 242, 263 (sh), 273 (sh), 284, 293, 326, 340 nm; ¹H NMR δ 3.38 (dd, 1H, 12-H, $J_{11,12} = 8.5$ Hz, $J_{12,13} = 6.5$ Hz), 4.22–4.30 (m, 1H, 3'-H), 4.30–4.35 (m, 1H, 13-H), 5.31 (d, 1H, 11-H, $J_{11,12} = 8.5$ Hz), 5.92 (d, 1H, 14-H, $J_{13,14} = 3.0$ Hz), 6.24 (dd, 1H, 1'-H, $J_{1',2'} = 6.0$ Hz, $J_{1',2'} = 7.0$ Hz), 7.46 (dd, 1H, 2-H, $J_{1,2} = 8.0$ Hz, $J_{2,3} = 7.5$ Hz), 7.74 (t, 1H, 3-H, $J_{2,3} = 7.5$ Hz, $J_{3,4} = 7.5$ Hz), 8.01 [s, 1H, 8-H(Gua)], 8.07 (dd, 1H, 6-H, $J_{5,6} = 7.5$ Hz, $J_{6,7} = 8.0$ Hz), 8.18 (dd, 2H, 8-H, 9-H), 8.29 (d, 1H, 7-H, $J_{6,7} = 8.0$ Hz), 8.41 (d, 1H, 1-H, $J_{1,2} = 8.0$ Hz), 8.54 (s, 1H, 10-H), 8.95 (d, 1H, 4-H, $J_{3,4} = 7.5$ Hz), 9.01 (d, 1H, 5-H, $J_{5,6} = 7.5$ Hz).

(+)-**(11S,12R,13R)-Trihydroxy-(14S)-N²dG-11,12,13,14-tetrahydro-DB[a,]P** [(+)-**syn-trans-N²dG**]: UV λ_{\max} 242, 280 (sh), 290, 297 (sh), 331, 344 nm; ¹H NMR δ 3.38–3.41 (m, 1H, 12-H), 3.80 (m, 1H, 4'-H), 4.20 (bs, 1H, 13-H), 4.31 (m, 1H, 3'-H), 4.84 (s, 1H, 11-H), 6.03 (bs, 1H, 14-H), 6.15 (bs, 1H, 1'-H), 7.27 (dd, 1H, 2-H, $J_{1,2} = 8.0$ Hz, $J_{2,3} = 7.0$ Hz), 7.71 (dd, 1H, 3-H, $J_{2,3} = 7.0$ Hz, $J_{3,4} = 8.0$ Hz), 8.03 [s, 1H, 8-H(Gua)], 8.07 (t, 1H, 6-H, $J_{5,6} = 8.0$ Hz, $J_{6,7} = 8.0$ Hz), 8.16 (s, 2H, 8-H, 9-H), 8.28 (d, 1H, 7-H, $J_{6,7} = 8.0$ Hz), 8.29 (s, 1H, 10-H), 8.68 (bd, 1H, 1-H), 8.97 (d, 1H, 4-H, $J_{3,4} = 8.0$ Hz), 9.04 (d, 1H, 5-H, $J_{5,6} = 8.0$ Hz).

(+)-**(11S,12R,13R)-Trihydroxy-(14R)-N7Gua-11,12,13,14-tetrahydro-DB[a,]P** [(+)-**syn-cis-N7Gua**]: UV λ_{\max} 242, 277 (sh), 286, 294 (sh), 328, 341 nm; ¹H NMR δ 3.85 (dd, 1H, 12-H, $J_{11,12} = 5.0$ Hz, $J_{12,13} = 7.5$ Hz), 3.95 (dd, 1H, 13-H, $J_{12,13} = 7.5$ Hz, $J_{13,14} = 4.0$ Hz), 4.94 (d, 1H, 11-H, $J_{11,12} = 5.0$ Hz), 6.97 [s, 1H, 8-H(Gua)], 7.27 (dd, 1H, 2-H, $J_{1,2} = 7.0$ Hz, $J_{2,3} = 8.0$ Hz), 7.41 (d, 1H, 14-H, $J_{13,14} = 4.0$ Hz), 7.62 (dd, 1H, 3-H, $J_{2,3} = 8.0$ Hz, $J_{3,4} = 7.5$ Hz), 8.06 (dd, 1H, 6-H, $J_{5,6} = 7.5$ Hz, $J_{6,7} = 8.0$ Hz), 8.16 (s, 2H, 8-H, 9-H), 8.29 (dd, 2H, 1-H, 7-H, $J_{1,2} = 7.0$ Hz, $J_{6,7} = 8.0$ Hz), 8.51 (s, 1H, 10-H), 8.84 (d, 1H, 4-H, $J_{3,4} = 7.5$ Hz), 8.96 (d, 1H, 5-H, $J_{5,6} = 7.5$ Hz).

(+)-**(11S,12R,13R)-Trihydroxy-(14S)-N7Gua-11,12,13,14-tetrahydro-DB[a,]P** [(+)-**syn-trans-N7Gua**]: UV λ_{\max} 241, 277 (sh), 289, 295 (sh), 328, 342 nm; ¹H NMR δ 3.70–3.80 (bs, 1H, 12-H), 4.00–4.10 (m, 1H, 13-H), 4.94 (d, 1H, 11-H, $J_{11,12} = 8.0$ Hz), 6.78 (d, 1H, 14-H, $J_{13,14} = 6.5$ Hz), 7.32–7.42 (m, 1H, 2-H), 7.62 (t, 1H, 3-H, $J_{2,3} = 7.5$ Hz, $J_{3,4} = 7.5$ Hz), 8.02 (t, 1H, 6-H, $J_{5,6} = 7.5$ Hz, $J_{6,7} = 7.5$ Hz), 8.08–8.15 [m, 3H, 8-H, 9-H, 8-H(Gua)], 8.24 (d, 2H, 1-H, 7-H, $J_{1,2} = 7.5$ Hz, $J_{6,7} = 7.5$ Hz), 8.47 (s, 1H, 10-H), 8.76 (d, 1H, 4-H, $J_{3,4} = 7.5$ Hz), 8.89 (d, 1H, 5-H, $J_{5,6} = 7.5$ Hz).

Results and Discussion

Synthesis and Isolation of Adducts. When both racemic and optically pure DB[a,]PDE were reacted with dG at 100 °C for 30 min, two types of adducts were isolated in high yield (Table 1): one formed by reaction of DB[a,]PDE at the benzylic C-14 position with the NH₂ group of dG (N²dG adducts) and the second formed by

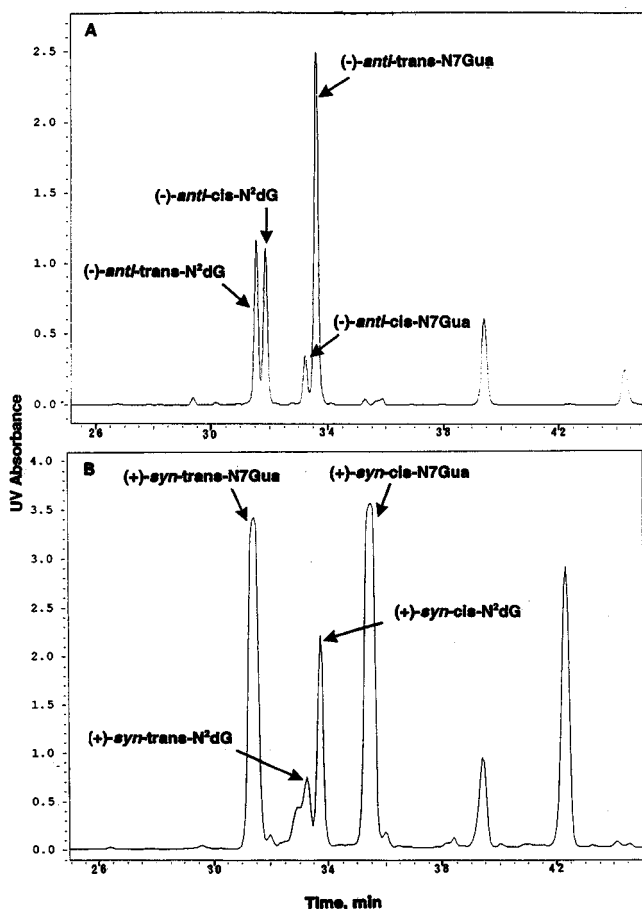


Figure 2. HPLC ($\text{CH}_3\text{CN}/\text{H}_2\text{O}$ gradient) profile of products obtained by reaction of (A) $(-)$ -*anti*-DB[a,l]PDE with dG and (B) $(+)$ -*syn*-DB[a,l]PDE with dG.

reaction of DB[a,l]PDE at C-14 with the N7 of dG leading to depurination (N7Gua adducts). Both (\pm) -*anti*-DB[a,l]PDE and (\pm) -*syn*-DB[a,l]PDE reacted with dG to give very good yields of *cis*- and *trans*-N²dG and -N7Gua adducts (Table 1, Figure 1). With $(-)$ -*anti*-DB[a,l]PDE, only one N7Gua adduct was isolated, and its yield was greater than those of the two N²dG adducts (Table 1, Figure 2A). With $(+)$ -*syn*-DB[a,l]PDE, the yield of N7Gua adducts was much greater than those of the N²dG adducts (Table 1, Figure 2B).

The N²dG adducts can be easily separated from the N7Gua adducts (Figure 1). However, efforts to further separate diastereomeric mixtures of *cis*- and *trans*-opened N7Gua adducts, or the four individual stereoisomers of optically active N²dG adducts obtained from racemic *anti*-DB[a,l]PDE (Scheme 1) and *syn*-DB[a,l]PDE (Scheme 2), were not successful under isocratic or gradient HPLC conditions. By using $(+)$ -*syn*- and $(-)$ -*anti*-DB[a,l]PDE, however, pure $(-)$ -*anti*-*cis*-N²dG, $(-)$ -*anti*-*trans*-N²dG, $(-)$ -*anti*-*trans*-N7Gua (Scheme 3, Figure 2A), $(+)$ -*syn*-*cis*-N²dG, $(+)$ -*syn*-*trans*-N²dG, $(+)$ -*syn*-*cis*-N7Gua, and $(+)$ -*syn*-*trans*-N7Gua (Scheme 4, Figure 2B) were obtained. The structures of all adducts were determined by NMR (Figures 3, 4, 7–9). The formulae of all the racemic N7Gua and stereoisomeric N²dG adducts were confirmed by FAB MS, and more confirmation was achieved by tandem MS, while the optically pure adducts were investigated by FLNS.

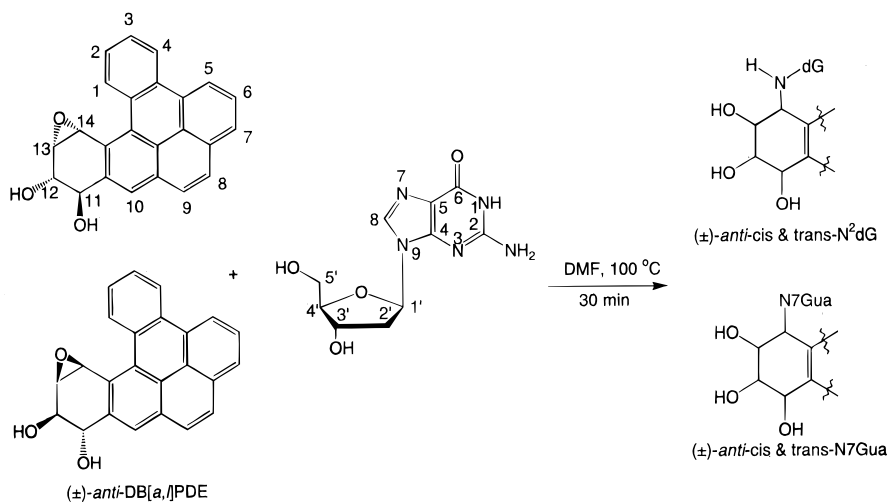
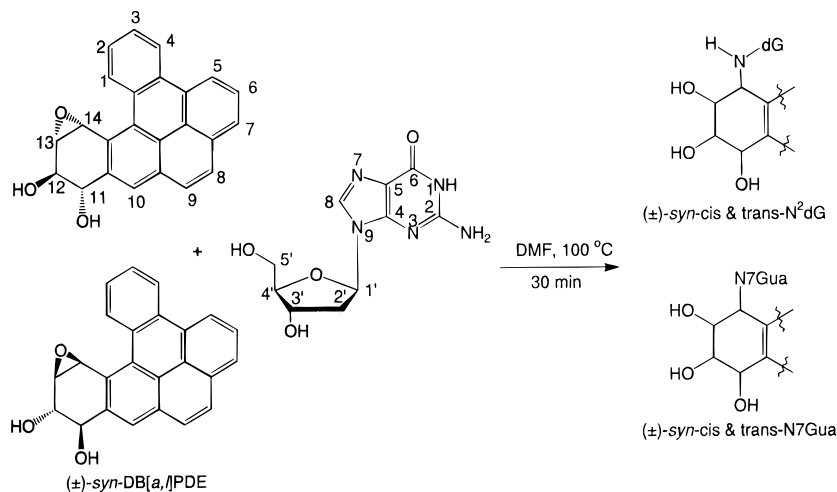
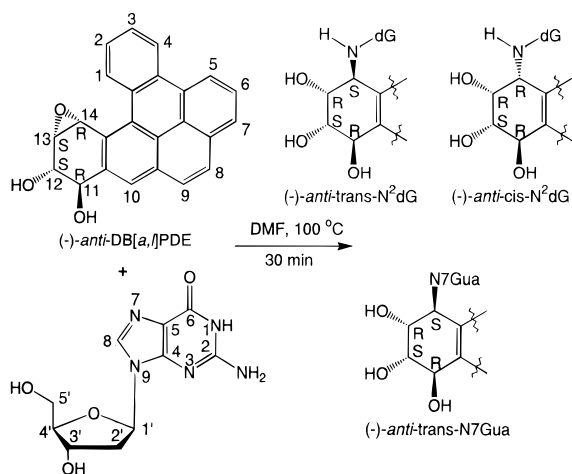
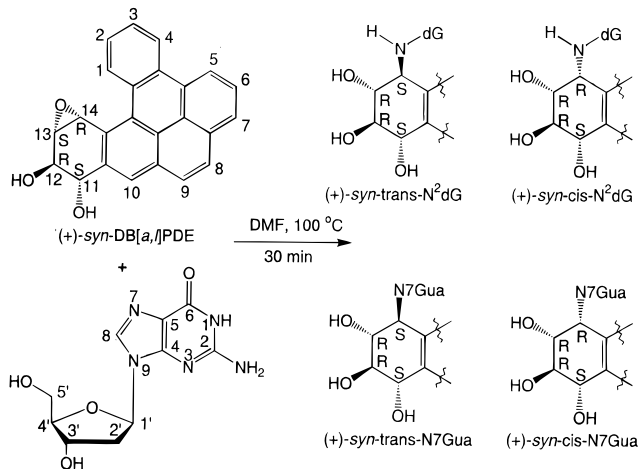
Structure Elucidation of Racemic Adducts. (1) (\pm) -*anti*-11,12,13-Trihydroxy-14-N²dG-11,12,13,14-

tetrahydro-DB[a,l]P [(±)-*anti*-*cis*- & -*trans*-N²dG]. The NMR spectrum (Figure 3A) of this mixture of four stereoisomers does not show different sets of chemical shifts, suggesting that the isomers exhibit almost identical NMR spectra. The absence of the NH₂ signal for dG around 7 ppm indicates that this group participates in the bond of dG to the dihydrodiol epoxide. The characteristic proton signals of the deoxyribose moiety further substantiate formation of the adduct at the exocyclic amino group. Furthermore, the signal of the H-14 proton of the DB[a,l]PDE moiety at 7.48 ppm (Table 2) is shifted significantly downfield compared to the signals of the other methine protons of the cyclohexenyl ring, indicating that the adduct has been formed between the C-14 of DB[a,l]PDE and the 2-NH₂ of dG. The signals of the remaining protons were assigned by a combination of ¹H NMR, two-dimensional chemical shift correlation spectroscopy (COSY), and D₂O treatment of exchangeable protons.

(2) (\pm) -*anti*-11,12,13-Trihydroxy-14-N7Gua-11,12,13,14-tetrahydro-DB[a,l]P [(±)-*anti*-*cis*- & -*trans*-N7Gua]. In the NMR spectrum of these adducts (Figure 3B), the two proton signals at 6.96 ppm, exchangeable with D₂O, show a chemical shift close to that of the amino group in dG (6.48 ppm, not shown). This indicates that the amino group is not involved in the formation of the adduct. The lack of a deoxyribose moiety in the adduct suggests that the bond between the dihydrodiol epoxide and dG occurs at N-7, with destabilization of the glycosidic bond and loss of the deoxyribose moiety. The chemical shifts of the remaining protons were assigned by ¹H NMR, COSY, and D₂O exchange. The substantial line broadening of the signals of all protons is attributable to the almost identical NMR spectra of the four stereoisomers, which could not be separated by HPLC.

(3) (\pm) -*syn*-11,12,13-Trihydroxy-14-N²dG-11,12,13,14-tetrahydro-DB[a,l]P [(±)-*syn*-*cis*- & -*trans*-N²dG]. The NMR spectrum of the title compounds (Figure 4A) shows two sets of proton signals, suggesting that the *cis* and *trans* stereoisomers can be identified. Assignment of the structure of these adducts is based on the lack of the NH₂ signal of dG (around 7 ppm) and the shift downfield of the H-14 proton, compared to the chemical shifts of the other methine protons of the cyclohexenyl ring. Furthermore, the proton signals of the deoxyribose are present. These data suggest that the adduct is formed by a bond between C-14 in the dihydrodiol epoxide moiety and the 2-NH₂ group of dG. Determination of the *cis*- and *trans*-opened adducts from the two sets of proton signals is based on the coupling constant $J_{13,14}$, which is larger for the *trans*- than *cis*-opened adducts (ref 5 and see below). It was found that *syn* isomers preferentially produce *cis*-opened adducts and *anti* isomers preferentially yield *trans*-opened adducts (5). Thus, in the two sets of signals, the major one is designated as deriving from the *cis*-opened adduct. The ratio of the *cis*- to *trans*-opened adducts is 70:30, as determined from peak areas.

(4) (\pm) -*syn*-11,12,13-Trihydroxy-14-N7Gua-11,12,13,14-tetrahydro-DB[a,l]P [(±)-*syn*-*cis*- & -*trans*-N7Gua]. The NMR spectrum of these adducts (Figure 4B) shows two sets of proton signals that are analogous to those of (\pm) -*syn*-*cis*- & -*trans*-N²dG (Figure 4A). The lack of deoxyribose signals and the presence of the 2-NH₂ proton signals indicate that these two diastereomers are the *syn*-*cis*- and *syn*-*trans*-opened N7Gua adducts. The smaller coupling constant $J_{13a,14a} = 3.5$ Hz (Table 2) is

Scheme 1. Reaction of (\pm)-*anti*-DB[a,*l*]PDE with dGScheme 2. Reaction of (\pm)-*syn*-DB[a,*l*]PDE with dGScheme 3. Reaction of (-)-*anti*-DB[a,*l*]PDE with dGScheme 4. Reaction of (+)-*syn*-DB[a,*l*]PDE with dG

designated as deriving from the *cis*-opened adduct and the larger $J_{13b,14b} = 4.5$ Hz (Table 2) from the *trans*-opened adduct. Integrating the peaks gives a ratio of *syn-cis* versus *syn-trans* adducts of 65:35.

Mass Spectra of the Racemic Adducts. FAB MS produces $[M + H]^+$ and $[M + Na]^+$ ions for the dihydrodiol epoxide adducts. Sufficient signal intensity was produced to enable exact-mass measurements of either the proto-

nated or sodiated molecules of the N²dG and N7Gua adducts (see Experimental Section). The elemental compositions were confirmed, as the measured masses were within 2.5–2.7 ppm of the theoretical masses for the four adducts.

In an effort to obtain structural information, the protonated or sodiated adducts were submitted to tandem mass spectrometry, and their collisionally activated decomposition (CAD) spectra were recorded. The dihy-

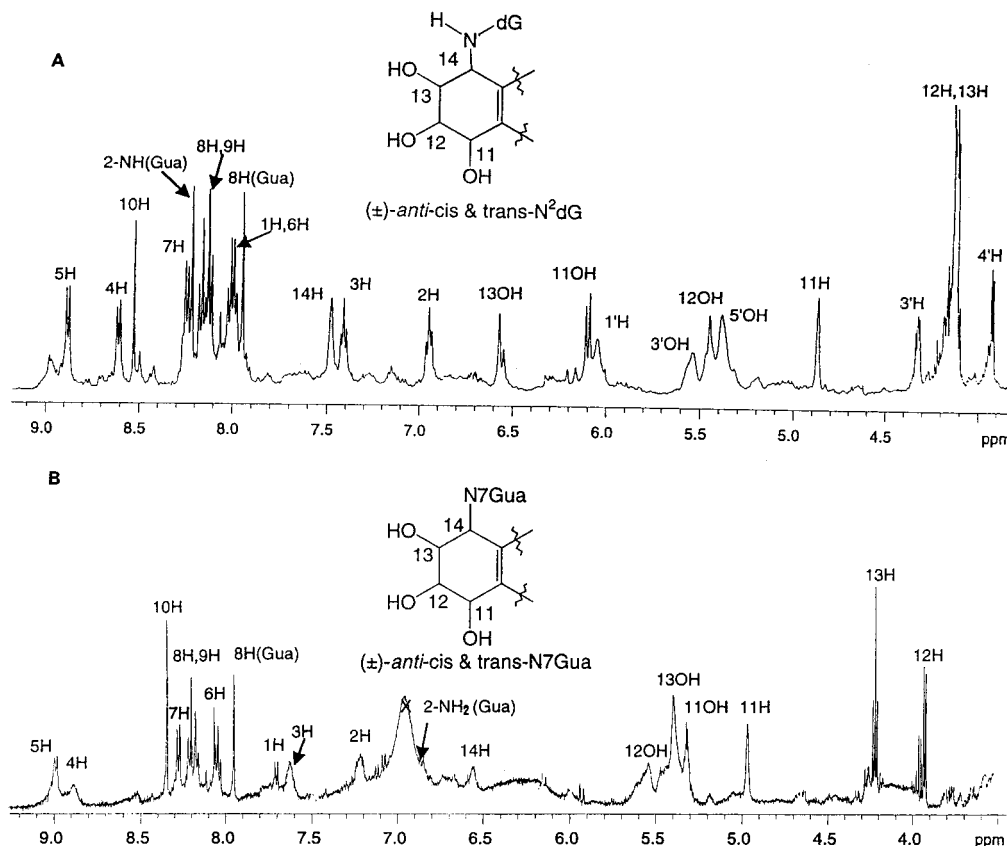


Figure 3. ^1H NMR ($\text{Me}_2\text{SO}-d_6$) of (A) (\pm) -*anti-cis*- & -*trans*- N^2dG and (B) (\pm) -*anti-cis*- & -*trans*- N^7Gua . Deoxyribose protons $2'$ - H_2 and $5'$ - H_2 in panel A resonate at higher fields (not shown); signal at 6.9 ppm in B (exchangeable with D_2O) is presumably an impurity derived from the HPLC column.

dihydrodiol epoxides do not desorb well, probably owing to the hydrophilicity of the three hydroxyl groups. Because of the poor sensitivity, we were able to obtain the CAD spectra only by using the array detector of the four-sector instrument. We present four spectra here to demonstrate that they are consistent with the proposed structures, but like the similar CAD spectra of dA adducts (5), the spectra are compound-class-specific, but not isomer-specific.

For the (\pm) -*anti-cis*- & -*trans*- N^2dG adducts, the CAD spectrum of the $[\text{M} + \text{H}]^+$ caused fragmentation of the molecules into their constituent parts (Figure 5A). Losses occur of the deoxyribose as $\text{C}_5\text{H}_8\text{O}_3$ and neutral Gua to give the ions of m/z 504 and 469, respectively. The latter is unexpected and may be due to migration of the PAH triol moiety from Gua to deoxyribose in the MS experiment. We also see formation of deoxyribose ion and protonated Gua at m/z 117 and 152, respectively. The triol moiety is expelled as an ion of m/z 353. There is a signature pattern for the triol moiety that consists of the fragment ions of m/z 353, 335, 317, 307, 289, 276/7, and 263. These ions are connected by losses of CO , H_2O , and portions of the six-membered ring containing the triol. An identical set of ions is formed in the fragmentation of DB[a,l]PDE-Ade and -dA adducts, although their relative abundances are different (5). Benzo[a]pyrene-7,8-dihydrodiol 9,10-epoxide adducts also give an analogous pattern of m/z 303, 285, 267, 257, 239, and 226/7 fragment ions (22), with m/z values 50 units (C_4H_2) lower than those of DB[a,l]P adducts.

The CAD or product-ion spectrum of the $[\text{M} + \text{H}]^+$ of (\pm) -*anti-cis*- & -*trans*- N^7Gua (Figure 5B) shows most of

the signature pattern for the triol (some ions are missing because there is a small gap in the center of the array detector). The presence of Gua is indicated by the fragment of protonated Gua at m/z 152.

To obtain CAD spectra of the (\pm) -*syn-cis*- & -*trans*- N^2dG and (\pm) -*syn-cis*- & -*trans*- N^7Gua adducts, we had to turn to $[\text{M} + \text{Na}]^+$ ions because the sample contained sufficient Na^+ to render the $[\text{M} + \text{H}]^+$ species poorly abundant. The spectrum (Figure 6A) of (\pm) -*syn-cis*- & -*trans*- N^2dG shows again that the dominant fragmentation is to disassemble the adduct into its constituent parts: $[\text{Gua} + \text{Na}]^+$ shifted to m/z 174 from m/z 152 for $[\text{Gua} + \text{H}]^+$ and ions formed by losses of deoxyribose (at m/z 526) and neutral Gua (at m/z 491). The latter ion suggests that N^2dG adducts may be susceptible to rearrangement of the PAH-triol moiety because the loss of the base is not seen for N^6dA adducts of this type (5). The pattern of peaks in the region of m/z 289, when amplified, is similar in ion membership, but not abundance, to the triol signature (m/z 335, 317, 307...), indicating that the Na^+ is bound preferentially with the deoxyribose/Gua portion of the molecule and is lost as part of the neutral moiety.

The CAD spectrum (Figure 6B) of the $[\text{M} + \text{Na}]^+$ of (\pm) -*syn-cis*- & -*trans*- N^7Gua illustrates more clearly the pattern of fragment ions in the m/z 289 region, and another version of this spectrum was published previously (23). One sees clearly that many of the fragment ions constitute the signature pattern of the PAH-triol and do not bear the Na^+ , indicating again a preference of Na^+ for the deoxyribose or base. A notable exception is the

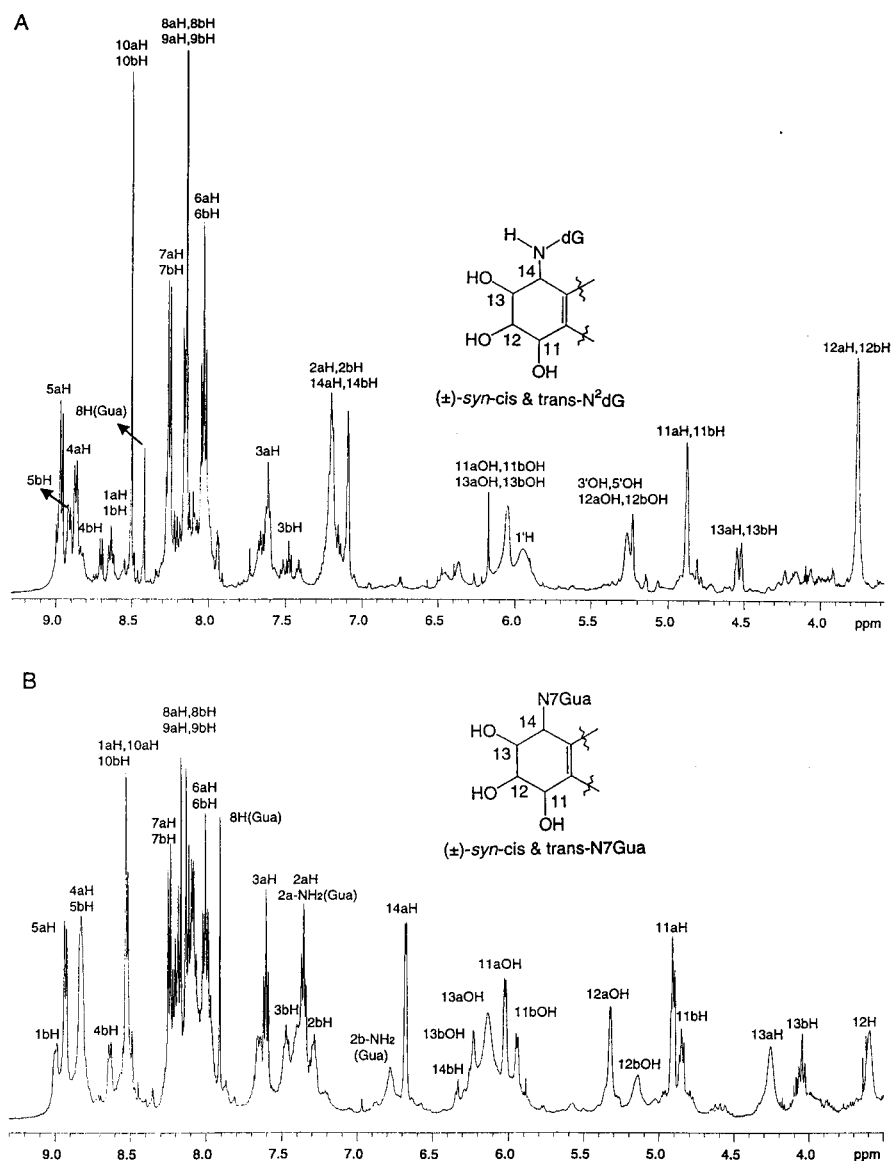


Figure 4. ^1H NMR ($\text{Me}_2\text{SO}-d_6$) of (A) (\pm) -*syn-cis*- & -*trans*-N²dG. The *cis*-opened N²dG is designated with the subscript a and the *trans*-opened with the subscript b. The deoxyribose protons 2'-H₂, 5'-H₂, and 4'-H resonate at higher fields (not shown). (B) ^1H NMR ($\text{Me}_2\text{SO}-d_6$) of (\pm) -*syn-cis*- & -*trans*-N⁷Gua. Description of the subscripts a and b is the same as in panel A.

abundant ion at m/z 375, which is the PAH-triol bound to Na^+ .

Structure Elucidation of (-)-*anti*-DB[a,*l*]PDE-dG and (+)-*syn*-DB[a,*l*]PDE-dG Adducts. The small amounts of the two dihydrodiol epoxides (-)-*anti*-DB[a,*l*]PDE and (+)-*syn*-DB[a,*l*]PDE available for synthesizing the dG adducts rendered challenging the elucidation of their structures. The NMR spectra were recorded in $\text{Me}_2\text{SO}-d_6/D_2\text{O}$ to sharpen the broad signals corresponding to the hydroxy and amino protons and, at the same time, to sharpen the signals corresponding to the C-H protons.

Of particular importance in elucidating the structures of the optically pure stereoisomers is an empirical rule that we developed by studying similar adducts obtained from the reaction of DB[a,*l*]PDE with dA: the *anti*-DB[a,*l*]PDE tend to produce more *trans*-opened adducts, whereas the *syn*-DB[a,*l*]PDE yield more *cis*-opened adducts. More important for establishing the structure of these adducts is the coupling constant $J_{13,14}$, which is relatively low for the *cis*-opened adducts and larger for the *trans*-opened adducts (5).

In the reaction of (-)-*anti*-DB[a,*l*]PDE with dG, three adducts were isolated and identified: namely the (-)-*anti-trans*-N²dG (17% yield), (-)-*anti-cis*-N²dG (12%), and (-)-*anti-trans*-N⁷Gua (43%; Table 1). The NMR spectra of these three adducts are shown in Figure 7. Assignment of the various proton signals was determined by ^1H NMR and COSY, and the rationale for distinguishing the N²-dG from the N⁷Gua adduct is based on the presence of the signals for the deoxyribose moiety in the former and their absence in the latter. The $J_{13,14} = 3.5$ Hz observed in spectrum 7A (Table 2) is small compared to $J_{13,14} = 8.0$ Hz in spectrum 7B. Therefore, the adduct with the smaller coupling constant is designated as the one that has 13-H and 14-H *cis* to each other, and thus, the absolute stereochemistry of the adduct must be 11*R*,12*S*,13*R*,14*R*. The adduct in Figure 7B, with $J_{13,14} = 8.0$ Hz, has the 13-H and 14-H *trans* to each other, and its absolute stereochemistry must be 11*R*,12*S*,13*R*,14*S*. Of the N⁷Gua adduct (Figure 7C), only one optically pure isomer was isolated; the other was obtained in trace amount (Figure 2A). The isolated adduct is designated

Table 2. Selected δ and J Values of DB[a,l]PDE Adducts Formed with dG

adduct	11-H	12-H	13-H	14-H	11-OH	12-OH	13-OH
(\pm)- <i>anti-cis</i> - & - <i>trans</i> -N ² dG	4.87 ($J_{13,14} = 2.0$ Hz)	4.11–4.17	4.11–4.17	7.48	6.10	5.35–5.60	6.57
(\pm)- <i>anti-cis</i> - & - <i>trans</i> -N7Gua	4.97 ($J_{12,13} = 6.5$ Hz, $J_{13,14} = 6.0$ Hz)	3.92	4.22	6.55	5.32	5.54	5.40
(\pm)- <i>syn-cis</i> - & - <i>trans</i> -N ² dG	4.88	3.75	4.50–4.57	7.08–7.25		5.21–5.31	
(\pm)- <i>syn-cis</i> - & - <i>trans</i> -N7Gua ^a	4.85 _b , 4.91 _a	3.59	4.05 _b , 4.26 _a	6.34 _b , 6.68 _a	5.94 _b , 6.02 _a	5.15 _b , 5.32 _a	6.13 _a , 6.23 _b
(-)- <i>anti-cis</i> -N ² dG	5.06 ($J_{11,12} = 8.5$ Hz, $J_{12,13} = 2.0$ Hz, $J_{13,14} = 3.5$ Hz)	4.13	4.32	6.54			
(-)- <i>anti-trans</i> -N ² dG	5.09 ($J_{11,12} = 8.5$ Hz, $J_{13,14} = 8.0$ Hz)	3.44	4.18	6.74			
(-)- <i>anti-trans</i> -N7Gua	4.97 ($J_{11,12} = 6.0$ Hz, $J_{12,13} = 2.0$ Hz, $J_{13,14} = 6.0$ Hz)	3.76	4.32	7.18			
(+)- <i>syn-cis</i> -N ² dG	5.31 ($J_{11,12} = 8.5$ Hz, $J_{12,13} = 6.5$ Hz, $J_{13,14} = 3.0$ Hz)	3.38	4.30–4.35	5.92			
(+)- <i>syn-trans</i> -N ² dG	4.84	3.38–3.41	4.20	6.03			
(+)- <i>syn-cis</i> -N7Gua	4.94 ($J_{11,12} = 5.0$ Hz, $J_{12,13} = 7.5$ Hz, $J_{13,14} = 4.0$ Hz)	3.85	3.95	7.41			
(+)- <i>syn-trans</i> -N7Gua	4.94 ($J_{11,12} = 8.0$ Hz, $J_{13,14} = 6.5$ Hz)	3.70–3.80	4.00–4.10	6.78			

^a Subscripts a and b refer to *cis*-opened adducts and *trans*-opened adducts, respectively.

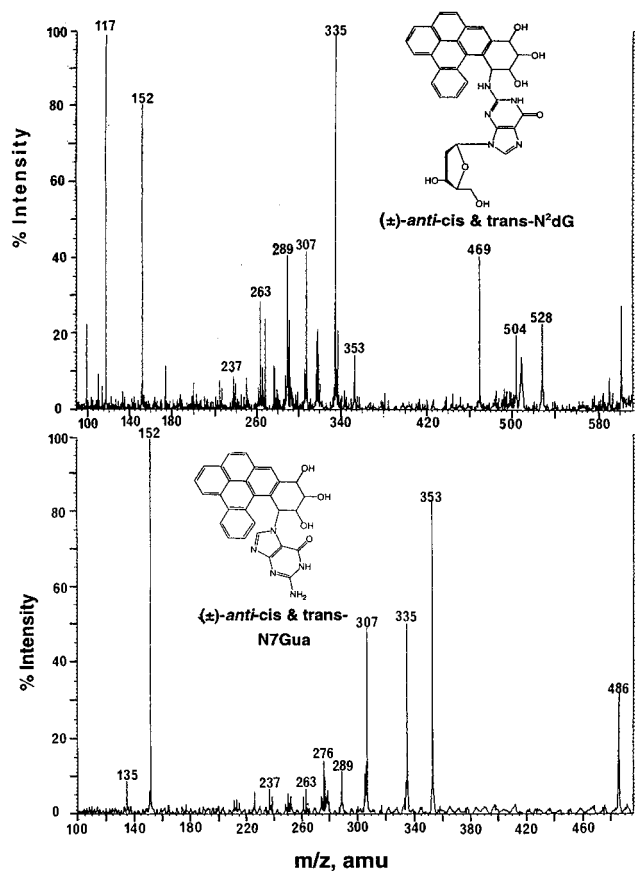


Figure 5. Portion of the CAD mass spectra of (A) $[M + H]^+$ ions of m/z 620 from (\pm)-*anti-cis*- & -*trans*-N²-dG and (B) $[M + H]^+$ ions of m/z 504 from (\pm)-*anti-cis*- & -*trans*-N7Gua.

as (-)-*anti-trans*-N7Gua because the yield was high, and the value for the coupling constant $J_{13,14} = 6.0$ Hz is also relatively high. Therefore, this adduct is designated with 11*R*,12*S*,13*R*,14*S*-absolute stereochemistry.

From reaction of (+)-*syn*-DB[a,l]PDE with dG, two N²-dG and two N7Gua adducts were obtained. From the small $J_{13,14} = 3.0$ Hz and the higher yield obtained for the isomer shown in Figure 8A, this adduct is designated as the (+)-*syn-cis*-N²dG, with 11*S*,12*R*,13*R*,14*R*-absolute stereochemistry. Thus, the adduct shown in Figure 8B must be the (+)-*syn-trans*-N²dG. Elucidation of the structure of the two N7Gua adducts obtained relies on

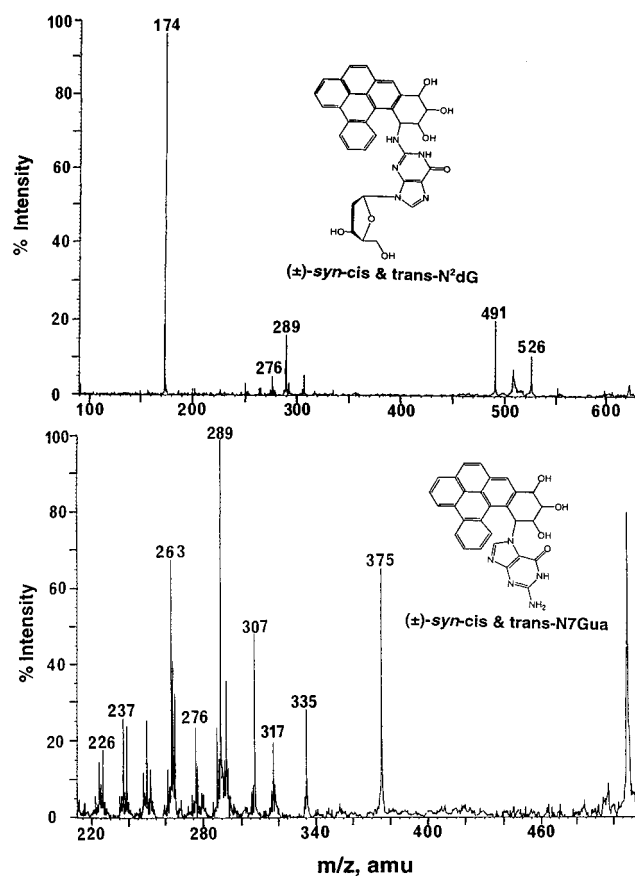


Figure 6. Portion of the CAD mass spectra of (A) $[M + Na]^+$ ions of m/z 642 from (\pm)-*syn-cis*- & -*trans*-N²-dG and (B) $[M + Na]^+$ ions of m/z 526 from (\pm)-*syn-cis*- & -*trans*-N7Gua.

the higher yield of the isomer designated as (+)-*syn-cis*-N7Gua (36%) with a relatively small $J_{13,14} = 4.0$ Hz (Figure 9A) versus the assigned (+)-*syn-trans*-N7Gua (22%) with $J_{13,14} = 6.5$ Hz.

Vibronically Excited FLN Spectra. The NLN fluorescence spectra at 77 K revealed that *anti-trans*-, *anti-cis*-, *syn-trans*-, and *syn-cis*-N²dG adducts exist mostly in folded-type conformation (17), with fluorescence origin bands at ~ 387 – 390 nm (unpublished results).

FLN multiplet origin structures for *anti-trans*- and *anti-cis*-N²dG adducts are shown in Figure 10; the FLN

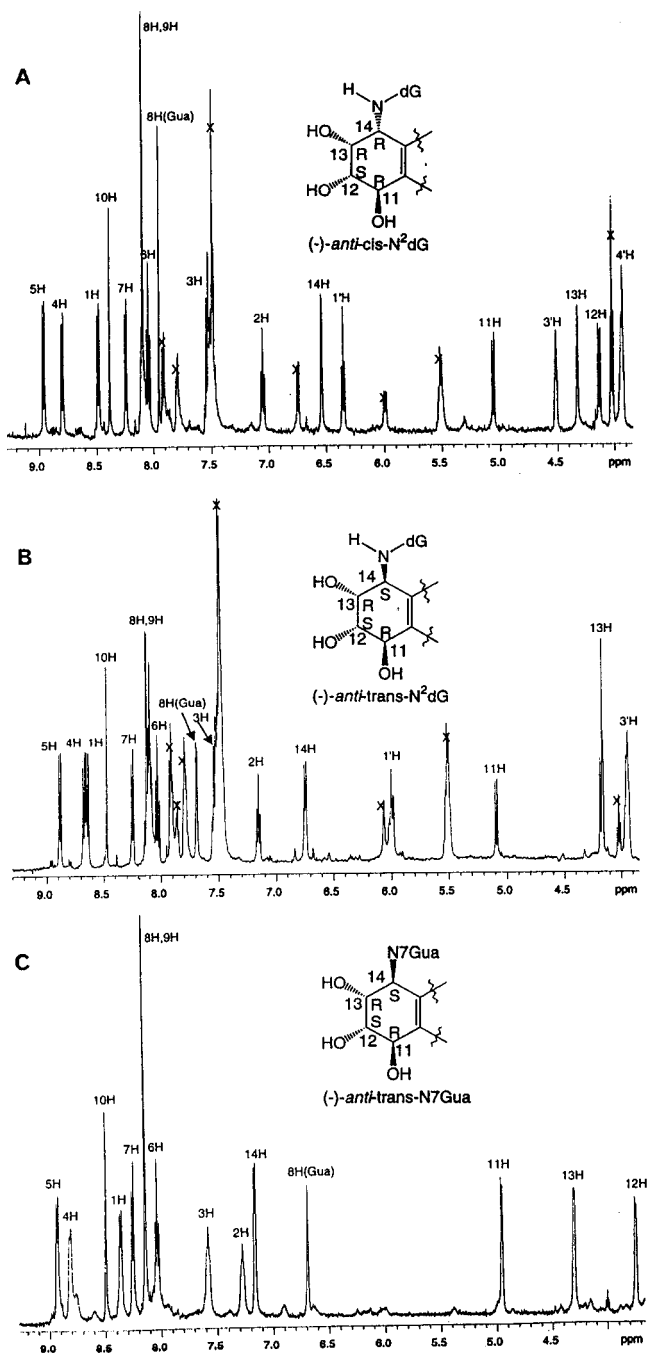


Figure 7. ¹H NMR (Me₂SO-*d*₆/D₂O) of (A) (-)-anti-cis-N²dG, (B) (-)-anti-trans-N²dG, and (C) (-)-anti-trans-N⁷Gua.

spectra in Figure 10A,B were acquired for two different excitation wavelengths: 379.0 and 376.0 nm, respectively. Spectra a and c were obtained for the *trans* isomer in glycerol/water at 4.2 K and spectra b and d for the *cis* isomer. The FLN peaks are labeled with their S₁ vibrational frequencies in cm⁻¹. For λ_{ex} = 376.0 nm (Figure 10B), the FLN spectra of *anti-trans*- and *anti-cis*-DB[a,β]-PDE-N²dG adducts are fairly similar; however, for λ_{ex} = 379.0 nm (Figure 10A), there are significant differences in the vibrational frequencies and intensities that enable spectral distinction of these two adducts. There are characteristic modes at 532, 545, 625, 635, and 698 cm⁻¹ for the *anti-trans*-N²dG adduct, whereas the *anti-cis*-N²dG adduct has modes at 536, 551, and 627 cm⁻¹. In addition, the relative intensities of the FLN peaks are different for these two adducts, with the higher frequency

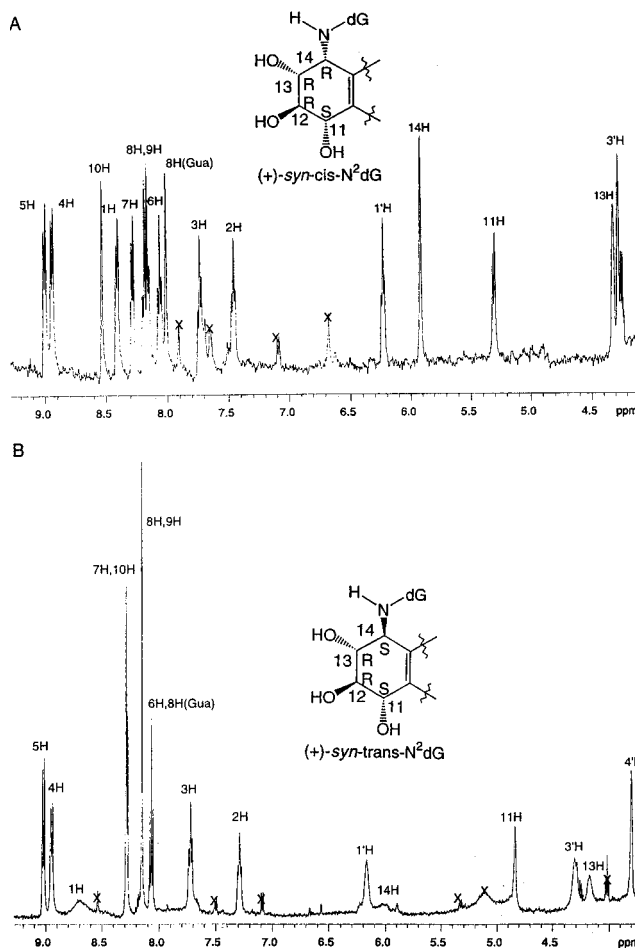


Figure 8. ¹H NMR (Me₂SO-*d*₆/D₂O) of (A) (+)-syn-cis-N²dG and (B) (+)-syn-trans-N²dG.

modes of *anti-trans*-N²dG being more intense than the corresponding modes for the *anti-cis*-N²dG adduct.

The same excitation wavelengths were used to generate FLN spectra for the *syn-trans*- and *syn-cis*-N²dG adducts, shown in Figure 11A,B, corresponding to different excitation wavelengths (λ_{ex} = 379.0 and 376.0 nm, respectively) that expose different regions of the vibronic spectrum. In Figure 11 the FLN peaks in the ~387–390-nm region correspond to excited-state vibrational modes of the major conformer II of these adducts. Spectra a and c are FLN spectra for *syn-trans*-N²dG in the glycerol/water glass at 4.2 K and spectra b and d for *syn-cis*-N²dG. Comparison of the spectra for these two adducts at the two excitation wavelengths reveals that *syn-cis* can be distinguished from its *syn-trans* stereoisomer on the basis of its characteristic vibrational modes at 543, 730, 865, 891, and 917 cm⁻¹; moreover, the modes at 690 and 882 cm⁻¹ are only observed for the *syn-trans* isomer. Because the FLN spectra for *syn-trans*- and *syn-cis*-N²dG in Figure 11 are significantly different from the spectra for the *anti-trans*- and *anti-cis*-N²dG adducts shown in Figure 10, differentiation of these four dG stereoisomeric adducts by FLNS is straightforward.

Conclusions

The reaction of (±)-*anti*-DB[a,β]PDE with dG gave two sets of adducts in good yield: (±)-*anti-cis*- & -*trans*-N²-dG and (±)-*anti-cis*- & -*trans*-N⁷Gua; both sets were mixtures of four stereoisomers that could not be sepa-

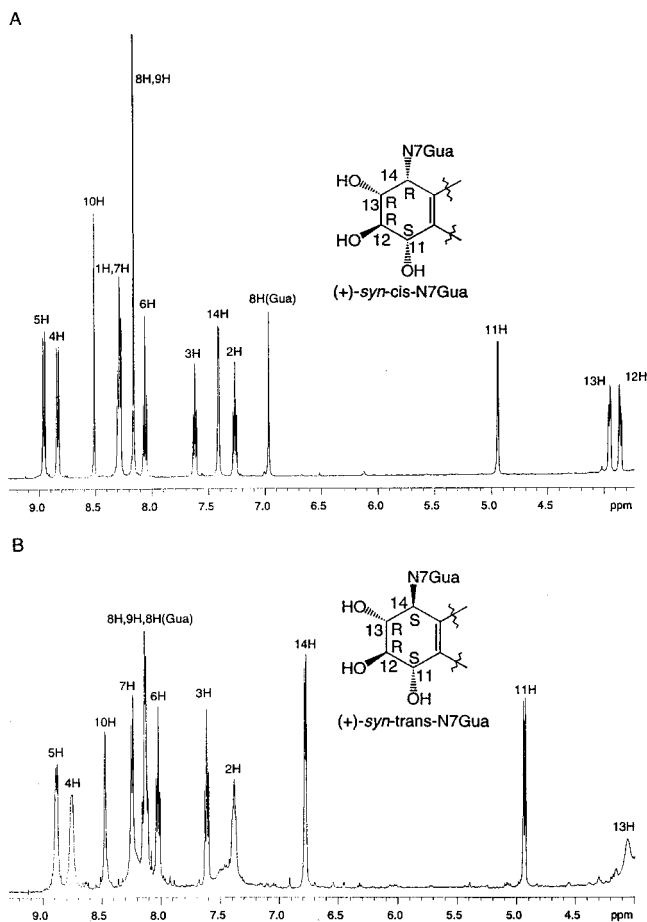


Figure 9. ^1H NMR ($\text{Me}_2\text{SO}-d_6/\text{D}_2\text{O}$) of (A) (+)-*syn-cis*-N7Gua and (B) (+)-*syn-trans*-N7Gua.

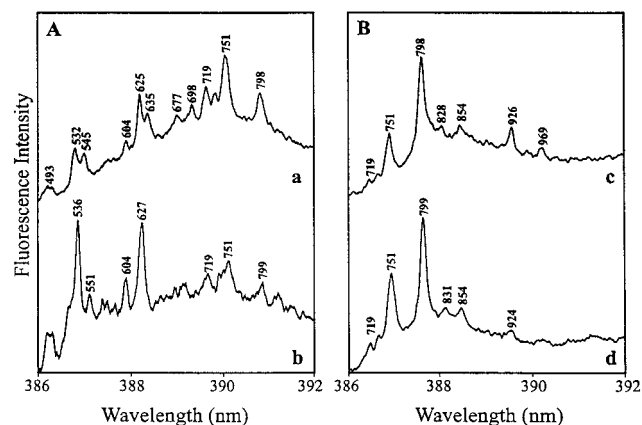


Figure 10. FLN spectra for *anti-trans*- and *anti-cis*-DB[a,]PDE- N^2dG adducts in 50/50 glycerol/water glass obtained for excitation wavelengths of (A) 379.0 nm and (B) 376.0 nm; $T = 4.2$ K. Spectra a and c are FLN spectra for *anti-trans*-DB[a,]PDE- N^2dG ; spectra b and d are for *anti-cis*-DB[a,]PDE- N^2dG . The FLN peaks are labeled with their excited-state vibrational frequencies in cm^{-1} .

rated on HPLC. Analogously, inseparable adducts were obtained in good yield from the reaction of (\pm)-*syn*-DB[a,]PDE with dG. The major difference between the four sets of adducts obtained from the two reactions is that the products from (\pm)-*syn*-DB[a,]PDE exhibited two sets of proton signals corresponding to the *cis* and *trans* diastereomers, whereas the adducts from (\pm)-*anti*-DB[a,]PDE did not. The structures of these adducts were determined by using a combination of NMR and FAB MS.

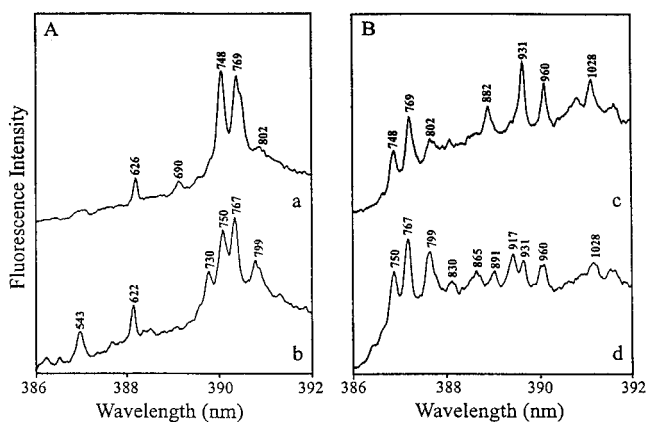


Figure 11. FLN spectra for *syn-trans*- and *syn-cis*-DB[a,]PDE- N^2dG adducts in 50/50 glycerol/water glass obtained for excitation wavelengths of (A) 379.0 nm and (B) 376.0 nm; $T = 4.2$ K. Spectra a and c are FLN spectra for *syn-trans*-DB[a,]PDE- N^2dG ; spectra b and d are for *syn-cis*-DB[a,]PDE- N^2dG . The FLN peaks are labeled with their excited-state vibrational frequencies in cm^{-1} .

Reaction of the optically pure ($-$)-*anti*-DB[a,]PDE and (+)-*syn*-DB[a,]PDE with dG afforded optically pure N^2dG and N7Gua adducts. The ($-$)-*anti*-DB[a,]PDE yielded more adducts *trans*-opened at the benzylic C-14, whereas (+)-*syn*-DB[a,]PDE afforded mainly *cis*-opened adducts. It was shown that FLNS possesses the necessary selectivity to distinguish the four stereoisomeric DB[a,]PDE-derived N^2dG adducts. With this technique, adducts from *anti*-DB[a,]PDE are easily distinguished from *syn*-DB[a,]PDE adducts, and the spectra of *trans*-opened adducts are different from those of *cis*-opened adducts. The FLN spectra acquired for these four stereoisomeric N^2dG adducts will serve future research projects as standards for positive identification of DB[a,]PDE-DNA stable adducts formed in biological systems.

Acknowledgment. This research was supported by Grants R01 CA49917 and P01 CA49210 from the National Cancer Institute. Core support at the Epplery Institute is provided by Grant P30-CA36727 from the National Cancer Institute and at the Washington University MS Research Resource by Grant P41-RR00954 from the National Center for Research Resources. Ames Laboratory is operated for the U.S. Department of Energy by Iowa State University under Contract No. W-7405-Eng-82. This research was also supported by the Deutsche Forschungsgemeinschaft (SFB 302).

References

- (1) Cavalieri, E. L., and Rogan, E. G. (1992) The approach to understanding aromatic hydrocarbon carcinogenesis. The central role of radical cations in metabolic activation. *Pharmacol. Ther.* **55**, 1083–1099.
- (2) Cavalieri, E. L., and Rogan, E. G. (1998) Mechanisms of tumor initiation by polycyclic aromatic hydrocarbons in mammals. In *The Handbook of Environmental Chemistry: PAHs and Related Compounds*, Vol. 3J (Neilson, A. H., Ed.) pp 81–117, Springer, Heidelberg.
- (3) RamaKrishna, N. V. S., Padmavathi, N. S., Cavalieri, E. L., Rogan, E. G., Cerny, R. L., and Gross, M. L. (1993) Synthesis and structure determination of the adducts formed by electrochemical oxidation of the potent carcinogen dibenzo[a,]pyrene in the presence of nucleosides. *Chem. Res. Toxicol.* **6**, 554–560.
- (4) Li, K.-M., Byun, J., Gross, M., Zamzow, D., Jankowiak, R., Rogan, E. G., and Cavalieri, E. L. (1999) Synthesis and structure determination of the adducts formed by electrochemical oxidation of dibenzo[a,]pyrene in the presence of adenine. *Chem. Res. Toxicol.* **12**, 749–757.

- (5) Li, K.-M., George, M., Gross, M. L., Seidel, A., Luch, A., Rogan, E. G., and Cavalieri, E. L. (1999) Structure elucidation of the adducts by fjord region dibenzo[*a,l*]pyrene 11,12-dihydrodiol 13,14-epoxides with deoxyadenosine. *Chem. Res. Toxicol.* **12**, 758–767.
- (6) Li, K.-M., Todorovic, R., Rogan, E. G., Cavalieri, E. L., Ariese, F., Suh, M., Jankowiak, R., and Small, G. J. (1995) Identification and quantitation of dibenzo[*a,l*]pyrene-DNA adducts formed by rat liver microsomes *in vitro*: Preponderance of depurinating adducts. *Biochemistry* **34**, 8043–8049.
- (7) Ralston, S. L., Lau, H. H. S., Seidel, A., Luch, A., Platt, K. L., and Baird, W. M. (1994) The potent carcinogen dibenzo[*a,l*]pyrene is metabolically activated to fjord-region 11,12-diol 13,14-epoxides in human mammary carcinoma MCF-7 cell structures. *Cancer Res.* **54**, 887–890.
- (8) Ralston, S. L., Seidel, A., Luch, A., Platt, K. L., and Baird, W. M. (1995) Stereoselective activation of dibenzo[*a,l*]pyrene to (-)-*anti*-(11*R*,12*S*,13*S*,14*R*)- and (+)-*syn*-(11*S*,12*R*,13*S*,14*R*)-11,12-diol-13,14-epoxides which bind exclusively to deoxyadenosine residues of DNA in the human mammary carcinoma cell line MCF-7. *Carcinogenesis* **16**, 2899–2907.
- (9) Jankowiak, R., and Small, G. J. (1991) Fluorescence line narrowing: a high-resolution window on DNA and protein damage from chemical carcinogens. *Chem. Res. Toxicol.* **4**, 256–269.
- (10) Rogan, E. G., Devanesan, P. D., RamaKrishna, N. V. S., Higginbotham, S., Padmavathi, N. S., Chapman, K., Cavalieri, E. L., Jeong, H., Jankowiak, R., and Small, G. J. (1993) Identification and quantitation of benzo[*a*]pyrene-DNA adducts formed in mouse skin. *Chem. Res. Toxicol.* **6**, 356–363.
- (11) Devanesan, P. D., RamaKrishna, N. V. S., Padmavathi, N. S., Higginbotham, S., Rogan, E. G., Cavalieri, E. L., Marsch, G. A., Jankowiak, R., and Small, G. J. (1993) Identification and quantitation of 7,12-dimethylbenz[*a*]anthracene-DNA adducts formed in mouse skin. *Chem. Res. Toxicol.* **6**, 364–371.
- (12) Kok, S. J., Posthumus, R., Bakker, I., Gooijer, C., Brinkman, U. A. Th., and Velthorst, N. H. (1995) Identification of benzo[*a*]pyrene tetrols by reversed-phase liquid chromatography coupled semi-on-line to fluorescence line-narrowing spectroscopy. *Anal. Chim. Acta* **303**, 3–10.
- (13) Marsch, G. A., Jankowiak, R., Suh, M., and Small, G. J. (1994) Sequence dependence of benzo[*a*]pyrene diol epoxide-DNA adduct conformer distribution: a study by laser-induced fluorescence/polyacrylamide gel electrophoresis. *Chem. Res. Toxicol.* **7**, 98–109.
- (14) Suh, M., Jankowiak, R., Ariese, F., Mao, B., Geacintov, N. E., and Small, G. J. (1994) Flanking base effects on the structural conformation of the (+)-*trans-anti*-benzo[*a*]pyrene diolepoxide adduct to N²-dG in sequence-defined oligonucleotides. *Carcinogenesis* **15**, 2891–2898.
- (15) Suh, M., Ariese, F., Small, G. J., Jankowiak, R., Liu, T.-M., and Geacintov, N. E. (1995) Conformational studies of the (+)-*trans*-, (-)-*trans*-, (+)-*cis*-, and (-)-*cis* adducts of *anti*-benzo[*a*]pyrene diolepoxide to N²-dG in duplex oligonucleotides using polyacrylamide gel electrophoresis and low-temperature fluorescence spectroscopy. *Biophys. Chem.* **56**, 281–296.
- (16) Ariese, F., Small, G. J., and Jankowiak, R. (1996) Conformational studies of depurinating DNA adducts from *syn*-dibenzo[*a,l*]pyrene diolepoxide. *Carcinogenesis* **17**, 829–837.
- (17) Jankowiak, R., Lin, C.-H., Zamzow, D., Roberts, K., Li, K.-M., and Small, G. J. (1999) Spectral and conformational analysis of deoxyadenosine adducts derived from *syn*- and *anti*-dibenzo[*a,l*]pyrene diol epoxides: Fluorescence studies. *Chem. Res. Toxicol.* **12**, 768–777.
- (18) *NIH Guidelines for the Laboratory Use of Chemical Carcinogens* (1981), NIH Publication No. 81-2385, U.S. Government Printing Office, Washington, DC.
- (19) Jankowiak, R., Ariese, F., Zamzow, D., Luch, A., Kroth, H., Seidel, A., and Small, G. J. (1997) Conformational studies of stereoisomeric tetrols derived from *syn*- and *anti*-dibenzo[*a,l*]pyrene diolepoxides. *Chem. Res. Toxicol.* **10**, 677–686.
- (20) Frank, H., Luch, A., Oesch, F., and Seidel, A. (1996) Assignment of absolute configuration to metabolically formed *trans*-dihydrodiols of dibenzo[*a,l*]pyrene by the exciton chirality method using a new red-shifted chromophore. *Polycyclic Aromat. Compd.* **10**, 109–116.
- (21) Luch, A., Seidel, A., Glatt, H. R., and Platt, K. L. (1997) Metabolic activation of the (+)-*S,S*- and (-)-*R,R*-enantiomers of *trans*-11,12-dihydroxy-11,12-dihydrodibenzo[*a,l*]pyrene: Stereoselectivity, DNA adduct formation, and mutagenicity in Chinese hamster V79 cells. *Chem. Res. Toxicol.* **10**, 1161–1170.
- (22) RamaKrishna, N. V. S., Gao, F., Padmavathi, N. S., Cavalieri, E. L., Rogan, E. G., Cerny, R. L., and Gross, M. L. (1992) Model adducts of benzo[*a*]pyrene and nucleosides formed from its radical cation and diol epoxide. *Chem. Res. Toxicol.* **5**, 293–302.
- (23) Cerny, R., Wellemans, J. M. Y., George, M., and Gross, M. L. (1994) The use of tandem mass spectrometry for the structure determination of adducts formed between DNA and dibenzo[*a,l*]pyrene. *Polycyclic Aromat. Compd.* **6**, 215–222.

TX980234K